Experimental Analysis of Nonlinear Impairments in Fibre Optic Transmission Systems up to 7.3 THz

Gabriel Saavedra, Mingming Tan, Daniel J. Elson, Lidia Galdino, Daniel Semrau, Md. A Iqbal, Ian D. Phillips, Paul Harper, Andrew Ellis, Benn C. Thomsen, Domaniç Lavery, Robert I. Killey, and Polina Bayvel

***Abstract*—An effective way of increasing the overall optical fibre capacity is by expanding the bandwidth used to transmit signals. In this paper, the impact of expanding the transmission bandwidth on the optical communication system is experimentally studied using the achievable rates as a performance metric. The tradeoffs between the use of larger bandwidths and higher nonlinear interference (NLI) noise is experimentally and theoretically analyzed. The growth of NLI noise is investigated for spectral bandwidths from 40 GHz up to 7.3 THz using 64-QAM and Nyquist pulse-shaping. Experimental results are shown to be in line with the predictions from the Gaussian-noise model showing a logarithmic growth in NLI noise as the signal bandwidth is extended. A reduction of the information rate of only 10% was found between linear and nonlinear transmission across several transmission bandwidths, increasing up to 7.3 THz. Finally, the power transfer between channels due to stimulated Raman scattering effect is analyzed showing up to 2-dB power tilt at optimum power for the largest transmitted bandwidth of 7.3 THz.**

***Index Terms*—GN model, nonlinear effects, optical fibre, optical fibre communications.**

I. Introduction

OPTICAL fibres are the fundamental transmission medium for modern communication systems. Among their most attractive features they present a low-loss region that spans tens of terahertz. To increase the amount of information transmitted over optical fibres, much research effort has been focused on extending the usable spectrum beyond the conventional C-band, covered by erbium doped fibre amplifiers (EDFAs). Techniques to increase the amplifier bandwidth have included parallel configurations of C and L-bands EDFAs [1], broadband seamless amplification using Raman amplifiers [2] and, recently, Bismuth and Thulium-doped fibre amplifiers to cover wavelengths longer than the L-band [3], [4]. Experimental demonstrations have shown systems capable of transmitting up to 70.4 Tb/s over 7600 km by using a parallel configuration of C and L-band (EDFAs) [5]. Additionally, reports of all-Raman amplified transmission show 9 Tb/s over 6000 km using 73 nm of bandwidth [6].

There are a number of physical effects which limit the achievable rates and overall throughput of optical fibre communications systems. Kerr nonlinearities affect the performance of high-speed optical communication systems, degrading the maximum signal-to-noise ratio (SNR) of the system and, therefore, the achievable information rates. Significant efforts have focused on the understanding and model the impact of nonlinear distortions on optical fibre system performance and achievable information rates. By treating the nonlinear distortions, often termed nonlinear interference (NLI) as additive noise, analytical models aim to provide the power spectral density of the NLI noise, which can be used to estimate system performance [7], [8]. The validity of these models has been assessed for several transmission fibre types and modulation formats via numerical simulations [7]. Due to the computational complexity required to simulate the propagation of large optical bandwidths using the Fourier split-step method, these validations have typically been limited to a small number of channels, e.g. 5 and 15 channels in [8], [9] respectively. Experimentally, several papers have shown good agreement with the model predictions [10]–[12], and results as a function of distance, at optimum signal power, for C-band systems also have been reported [13]. However, a detailed experimental study analysing a variety of bandwidths in the nonlinear regime has not been carried out to date. Associated with the increase of bandwidth beyond C-band is the growth of stimulated Raman scattering, which manifests itself as power transfer between channels and needs to be investigated in the context of increasing the usable optical fibre spectral range. To date there have been no detailed studies of this for high-capacity coherent optical transmission systems.

In our previous work [14] the accumulation of NLI noise for ultra-wideband fibre transmission up to 7.3 THz was experimentally and theoretically studied. In this work these results are extended to analyse the trade-off between an increase in the transmission bandwidth and growth of nonlinear effects

Manuscript received June 16, 2017; revised August 17, 2017 and September 28, 2017; accepted September 29, 2017. Date of publication October 5, 2017; date of current version October 25, 2017. This work was supported in part by Becas Chile, in part by UK EPSRC UNLOC Programme under Grant EP/J017582/1, in part by FP7 ITN Programme ICONE(608099), and in part by the Royal Academy of Engineering under the Research Fellowships scheme. *(Corresponding author: Gabriel Saavedra.)*

G. Saavedra, D. J. Elson, L. Galdino, D. Semrau, D. Lavery, R. I. Killey, and P. Bayvel are with the Optical Networks Group, Department of Electronic and Electrical Engineering, University College London, Bloomsbury, London WC1E 7JE, U.K. (e-mail: gabriel.mondaca.14@ucl.ac.uk; uceegsa@ucl.ac.uk; lgaldino@ee.ucl.ac.uk; uceedfs@ucl.ac.uk; d.lavery@ee.ucl.ac.uk; r.killey@ucl.ac.uk; p.bayvel@ucl.ac.uk).

M. Tan, Md. A. Iqbal, I. D. Phillips, P. Harper, and A. D. Ellis are with the Aston Institute of Photonic Technologies, Aston University, Birmingham B4 7ET, U.K. (e-mail: m.tan1@aston.ac.uk; iqbalm7@aston.ac.uk; i.phillips@aston.ac.uk; p.harper@aston.ac.uk; andrew.ellis@aston.ac.uk).

B. C. Thomsen was with the Optical Networks Group, Department of Electrical and Electronic Engineering, University College London, Bloomsbury WC1E 7JE. He is now with Microsoft Research, Cambridge CB1 2FB, U.K. (e-mail: Benn.Thomsen@microsoft.com).

Color versions of one or more of the figures in this paper are available online at http://ieeexplore.ieee.org.

Digital Object Identifier 10.1109/JLT.2017.2760138

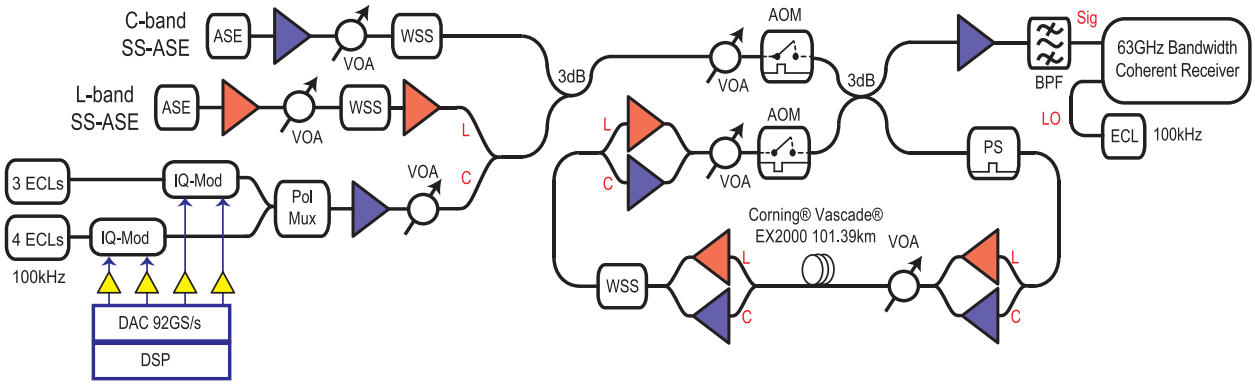

Fig. 1. Experimental setup used to investigate nonlinear distortions in wide bandwidth transmission.

using the mutual information (MI) as a performance metric. This allowed us to obtain an estimate of the highest achievable information rate (AIR) in the system under test. In addition, the degradation of the AIR and the total system throughput as a function of the total transmitted bandwidth were experimentally studied for the first time. The channel under test was 40 GBd Nyquist-shaped dual polarization 64-ary quadrature-amplitude modulated (DP-64QAM), and the total transmitted spectral bandwidth was varied between 40 GHz and 7.3 THz, over distances up to 2500 km. The transmission performance was also analysed using the GN-model which was extended to include transceiver noise. Additionally, the power transfer between signals due to stimulated Raman scattering is studied.

II. Experimental Setup and Methodology

This section describes the experimental setup used to analyse nonlinear distortion and its evolution as the transmission bandwidth is increased, together with the theoretical model used to estimate the system performance.

A. Experimental Setup

A schematic of the experimental setup used is shown in Fig. 1. Seven external cavity lasers (ECLs), spaced at 41 GHz, with a nominal linewidth of 100 kHz were connected to two independent IQ optical modulators driven by the amplified outputs from 92 GS/s digital-to-analogue converters (DACs). A digital root raised cosine (RRC) filter with 0.1 % roll-off was used to spectrally shape the signals and pre-emphasis was applied to overcome the electrical response of the transmitter components, including limited bandwidth of electrical amplifiers and optical modulators. The modulated channels were combined and then polarization multiplexed (PM) using a PM emulator to form a 7×40 GBd DP-64QAM signal. Spectrally-shaped, amplified spontaneous emission (SS-ASE) noise was used to emulate additional interfering channels, allowing a range of transmission bandwidths to be investigated. SS-ASE was generated separately in each transmission band by a pair of EDFAs and subsequently shaped by individual wavelength selective switches (WSS). The WSS was used to create a notch in the SS-ASE, with an extinction ratio of 35 dB, to couple the modulated signals without compromising their optical signal-to-noise ratio.

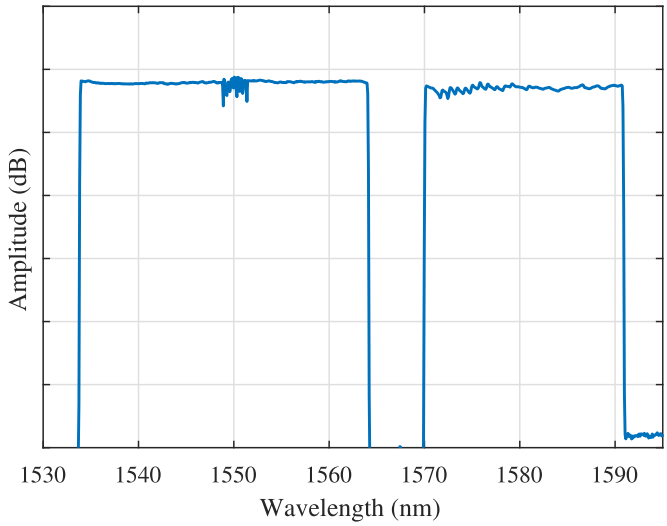

Fig. 2. Optical spectrum of the transmitted signal.

The validity of this methodology was verified in [15], [16], showing that this technique provides a conservative measure of system performance. Further, this technique has been used in [17] to study the achievable rates using real time processing in transatlantic systems. The total propagated bandwidths used in this work were 40, 280, 600, 1200, 2500, 4100 and 7300 GHz. The C-band was occupied from 1535 to 1566 nm and the L-band was occupied from 1570 to 1591 nm. A gap of 4 nm between the C and L-bands was necessary to perform optical amplification in each band, which can be seen in Fig. 2. Since no optical power is present in that region of the spectrum it does not contribute to the increase of NLI noise. The optical spectrum of the received signal of 7.3 THz was measured with a resolution of 0.1 nm, and is shown in Fig. 2. The 7 modulated channels are centred at 1550 nm, placed in the notch carved in the SS-ASE. For transmission, a single-span recirculating optical fibre loop was used. A single span loop underestimates the transmission system performance in the linear regime compared to a straight-line system or a multi-span loop. This is due to the extra ASE noise introduced by the EDFA used to overcome the losses from the passive components. Optical amplification within the transmission loop was carried out in parallel for the C- and L-band using EDFAs with nominal

noise figures of 5 and 6.5 dB, respectively. The loop consisted of two acousto-optic modulators (AOMs), a loop synchronous polarization scrambler (PS), and three pairs of EDFAs to overcome fibre and component losses. The maximum output of the C and L-band EDFAs were 33 and 23 dBm respectively, hence the maximum signal power per channel for C+L-band transmission was limited to 4 dBm in order to maintain the power spectral density (PSD) between both transmission bands. The fibre span used was 101 km of Corning Vascade EX2000 Fiber with an attenuation coefficient of 0.160 dB/km, dispersion parameter of 20.2 ps/nm·km and nonlinear coefficient of 0.85 $\mathrm{W^{-1}km^{-1}}$. The signal power into the fibre span was controlled using an variable optical attenuator and measured using a 2% tap and an optical spectrum analyser with a resolution of 0.1 nm. A WSS was used in the loop as an adjustable gain flattening filter to compensate for any gain tilt in the system. The WSS in the loop was configured for maximum spectral flatness. The filter shapes were created by measuring the optical spectrum at the output of every recirculation and applying the inverse profile to the WSS. This was done for every transmission distance at optimum launch power for the 7.3 THz signals. Subsequently, at 1010 km the filters were updated, again using the received optical spectrum, for every signal launch power. Finally, the same filters were used for the transmission of smaller bandwidths. At the receiver the optical signal was optically amplified and a band-pass filter of 120 GHz, centred at 1550 nm, was used to select the channel of interest, allowing the joint detection of three 40 GBd channels. A separate ECL was used as the local oscillator, and detection was carried out by balanced photodetectors with 70 GHz electrical bandwidth and sampled by a real-time digital oscilloscope with an analogue electrical bandwidth of 63 GHz at 160 GSa/s. Chromatic dispersion compensation was subsequently performed before filtering the signal using a matched RRC filter. The signals were equalised using a radius directed equaliser [18], with the constant modulus algorithm equaliser used for pre-convergence [19]. The carrier phase was estimated per polarisation using a decision-directed phase estimation algorithm [20]. Gram-Schmidt orthogonalisation [21] was performed in order to correct for any sub-optimal phase bias in the transmitter IQ modulators. SNR was ideally estimated as the ratio between the variance of the transmitted symbols $E[|X|^2]$, with $X \in \{x_i\}_{i=1}^{m}$, and the variance of the noise $\sigma^2 = E[|X-Y|^2]$, where Y is the random variable representing the received symbols after DSP. Finally, the mutual information (MI) was calculated per polarization, using a mismatched decoder approach with a Gaussian auxiliary channel [22, eq. (14)]. The integration was performed using the Monte Carlo approximation as follows:

$$\mathrm{MI} = \log_2 m - \frac{1}{mN_s}\sum_{i=1}^{m}\sum_{n=1}^{N_s} \log_2 \sum_{j=1}^{m} \exp\left[-\frac{|x_i - x_j|^2 + 2\,\mathrm{Re}\left\{(x_i - x_j)^*(y_i[n] - x_i)\right\}}{\sigma^2}\right], \tag{1}$$

where m is the constellation cardinality, N_s is the number of received samples, $y_i[n]$ is the n-th sample of the random variable Y corresponding to the transmitted symbol x_i.

B. The System Model

Theoretical models of the optical fibre channel able to predict system performance have been extensively investigated, becoming an important tool in system design. Among them, the GN-model allows for the estimation of the NLI noise power present in an optical communication system, and has been shown to be accurate in dispersive, long-haul links. Key assumptions of the model are that the transmitted signal behaves statistically as a Gaussian process, that nonlinear distortions can be modelled as additive Gaussian noise, and they are treated as a small perturbations on the signal. From [7] the PSD of the noise at the end of a transmission link can be expressed as:

$$\begin{aligned} G_{\mathrm{NLI}}(f) &= \frac{16}{27}\gamma^2 L_{\mathrm{eff}}^2 \\ &\cdot \int_{-\infty}^{\infty}\int_{-\infty}^{\infty} G_{\mathrm{WDM}}(f_1) G_{\mathrm{WDM}}(f_2) G_{\mathrm{WDM}}(f_1+f_2-f) \\ &\cdot \rho(f_1,f_2,f)\cdot\chi(f_1,f_2,f) df_2 df_1, \end{aligned} \tag{2}$$

where γ corresponds to the fibre nonlinear coefficient, L_{eff} is the effective nonlinear beating length, $G_{\mathrm{WDM}}(f)$ is the PSD of the transmitted signal, $\rho(f_1,f_2,f)$ is the normalized four wave mixing efficiency and $\chi(f_1,f_2,f)$ is the phased-array factor responsible for the coherent accumulation of NLI noise with distance. Alternatively, a closed-form expression was presented to calculate the NLI coefficient for a single span, defined as [7]:

$$G_{NLI}(0) \approx \frac{8}{27}\gamma^2 G_{WDM}^3 \frac{log_e(\pi^2 \beta_2 L_{eff,a} B_{WDM}^2)}{\pi \beta_2 L_{eff,a}}, \tag{3}$$

where B_{WDM} corresponds to the signal bandwidth.

Equation (2) was used to calculate the NLI noise power and used to estimate the theoretical performance of the system under test. The received SNR was calculated as the ratio between the signal power and the sum of the ASE noise, NLI noise and transceiver noise as detailed in [23]:

$$\mathrm{SNR} = \frac{P}{NP_{\mathrm{ASE}} + \eta P^3 + P(\mathrm{SNR_{TR}})^{-1}}, \tag{4}$$

where P is the signal power, N the number of spans, P_{ASE} the ASE noise power and η the NLI coefficient obtained by numerically integrating (2) over the signal bandwidth. The noise introduced by the transceiver subsystem is defined as $\mathrm{SNR_{TR}}$, and corresponds to the maximum SNR that can be achieved in the transmission system in the absence of NLI noise and ASE noise. This was experimentally found by measuring the SNR in the back-to-back configuration without noise loading. In order to quantify the total ASE noise in the system, the optical signal-to-noise ratio (OSNR) was measured at the receiver after transmission of 10 recirculations at optimum signal power for each transmitted bandwidth by turning off the set of 4 ECLs from the transmitter. This way the contributions from all the EDFAs within the recirculating loop were included in term P_{ASE}. (4) allows calculation of the SNR for an optical system of different

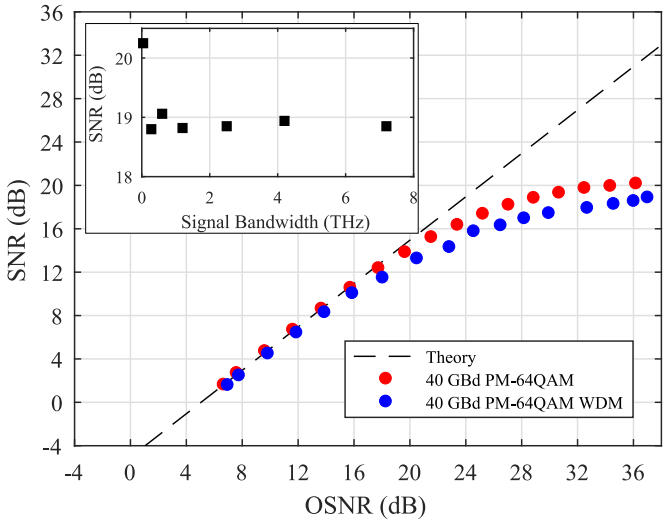

Fig. 3. Back-to-back characterisation of the transceiver subsystem. Received SNR as a function of signal OSNR measured in 0.1 nm bandwidth. Red markers represent single channel system and blue markers WDM system. Inset shows the maximum SNR in back-to-back configuration, corresponding to $\mathrm{SNR}_{\mathrm{TR}}$, for all the signal bandwidths under investigation.

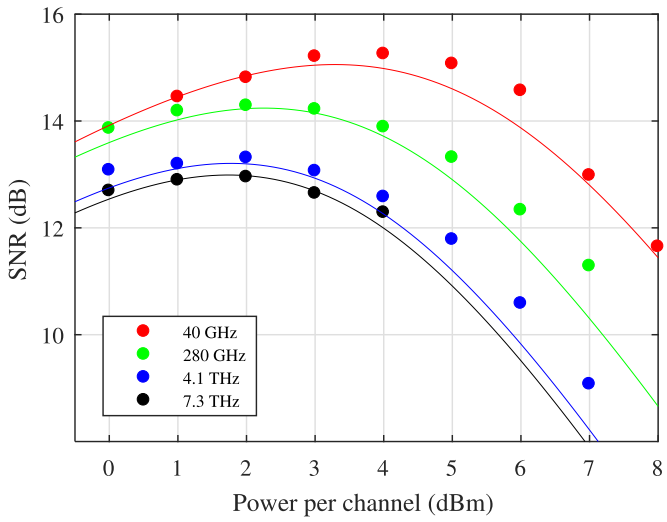

Fig. 4. Performance of the transmission system for different transmitted bandwidths after 1010 km, solid lines represent the predictions obtained using (4) and markers correspond to experimental data.

bandwidths by changing the bandwidth of $G_{\mathrm{WDM}}(f)$ in (2). For bandwidths covering up to the C-band this was increased continuously assuming Nyquist shaped and spaced signals. For signals covering the C and the L-band the total spectrum was approximated using two rectangles covering each band with a separation of 4 nm to resemble the behaviour of the experimental test-bed, as seen in Fig. 2.

III. Results and Discussion

A. Back-to-Back Characterisation

In order to use (4) to estimate the performance of the transmission system, the $\mathrm{SNR}_{\mathrm{TR}}$ needs to be characterised over the entire bandwidth of interest.

Back-to-back performance of the system was experimentally characterized as a function of the signal OSNR. This was carried out by coupling an ASE source before the coherent receiver, allowing the control of the signal OSNR. The characterisation is shown in Fig. 3, where the received SNR is plotted as a function of the signal OSNR. A linear relationship was observed for OSNR values below 16 dB, and the received SNR saturated at 20 dB for a single channel and 19 dB in the WDM case. Beyond this point increasing the OSNR does not increase the received SNR, mainly due to the noise introduced by the electrical components of the transceiver, such as the limited effective number of bits (ENOB) of the DAC and sampling scope, and the use of electrical amplifiers to drive the optical modulators. The inset of Fig. 3 shows the maximum SNR in the back-to-back configuration for all the signal bandwidths under investigation. The bandwidths correspond to 40, 280, 600, 1200, 2500, 4100 and 7300 GHz as described in the previous section. A SNR of 20.1 dB was obtained when a single channel of 40 GBd was generated and detected, however, a penalty of approximately 1 dB was found when transmitting a larger bandwidth. This penalty arises from the use of digital oscilloscopes with interleaved analogue-to-digital converters (ADC) for the sampling of large bandwidth signals. This penalty is observed when the received signal occupies the entire oscilloscope bandwidth. The average received SNR for WDM signals is 18.9 dB, and this values was used as $\mathrm{SNR}_{\mathrm{TR}}$ to calculate SNR using (4). The high extinction ratio of 35 dB from the WSS allows for the OSNR of the transmitter, of 35 dB as seen in Fig. 3, to be maintained after combining the signal with the SS-ASE. Thus, transmission of signals occupying bandwidths beyond 280 GHz, was not affected by the introduction of additional penalties due to ASE accumulation.

B. NLI Induced Impairments

In order to analyse the accumulation of NLI noise over different bandwidths the system performance was evaluated after transmission over a fixed distance of 1010 km, corresponding to 10 spans. This distance provides enough accumulated dispersion for the GN model assumptions on signal Gaussianity to be valid. The signal launch power per channel was varied between -1 and 7 dBm and SNR of the received signal was measured. The SNR as a function of the signal launch power for different transmitted bandwidths is shown in Fig. 4. In the linear regime, a small difference in receiver SNR can be observed among the different transmitted bandwidths, this is due to the power equalization process carried out by the WSS within the recirculating loop. As the propagated bandwidth is increased, the tilt from the EDFAs becomes larger and the WSS must intervene in an increasingly manner to correct the tilt, leading to a small difference in the overall loop loss. Towards the highly nonlinear regime, for a fixed signal launch power, a penalty in SNR can be observed with increase of transmission bandwidth, as expected from the growth of the NLI noise power. For instance, at a launch power of 4 dBm per channel, the difference observed in SNR between the transmission bandwidths of 40 GHz and 7.3 THz

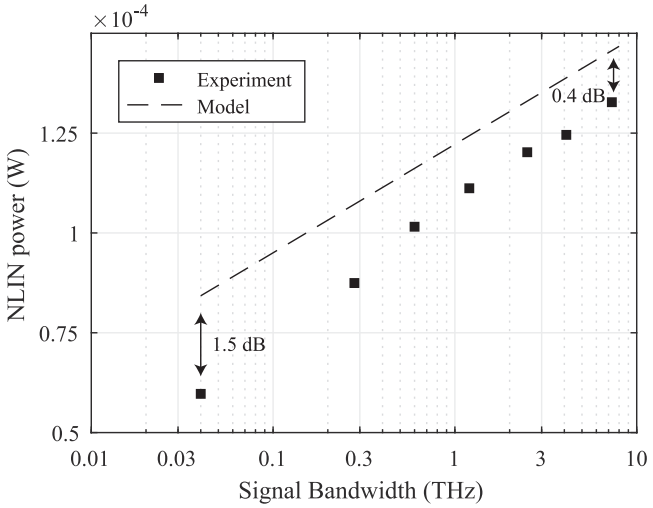

Fig. 5. Growth of NLI noise power as the signal bandwidth is increased evaluated after transmission of 1010 km. Markers show the experimentally obtained data and dashed line the results predicted by the model.

is approximately 2.7 dB. Fig. 4 additionally depicts the theoretical performance of the system (solid lines) for all the evaluated bandwidths obtained using (4). One well-known limitation of the GN-model is the assumption is that the transmitted signal behaves statistically like Gaussian noise, neglecting this way modulation format dependence of the NLI noise. Even though this has been addressed in the literature [24], [25] it leads to additional complexity when computing the NLI noise power, specially for large bandwidth systems. This limitation is translated in an overestimation of the NLI noise by the GN model compared to the use of QAM modulated signals, and therefore a underestimation of the system performance in the nonlinear regime. Using the experimental data, the model was confirmed to give a slightly pessimistic prediction of performance in the nonlinear regime for the all evaluated bandwidths. At optimum signal power and in the absence of transceiver noise, the difference between the predictions of the GN model and the experimental data is reduced according to the rule (as seen in [7, eq. (32)]):

$$\Delta\text{SNR}[\text{dB}] \approx -\frac{1}{3}\Delta\eta[\text{dB}], \tag{5}$$

therefore, a closer agreement between the model and the experimental data is seen at optimum signal launch power with respect to higher launch powers.

In order to analyse the growth of the NLI noise as a function of transmitted bandwidth, the NLI noise power was obtained from the experimental results at a distance of 1010 km. To carry this out the following method was used: Firstly, the received SNR was measured in the linear regime (at -8 dBm per channel), where NLI noise is negligible. This way the linear noise (P_{ASE}) was extracted. Subsequently, to estimate the nonlinear noise, the received SNR was measured at high signal launch power (+4 dBm per channel) and the NLI noise power was extracted from (4). Fig. 5 shows the NLI noise power as a function of transmitted bandwidth. From (3), is seen that the NLI coefficient is proportional to the logarithm of the total transmitted bandwidth B_{WDM}. This same trend can be observed in Fig. 5, where the NLI noise power grows in a logarithmic law as the bandwidth is increased. The dashed line represents the predictions from the model presented in (2). An offset between the model and the experiment can be seen due to a main reasons. The GN-model assumes that the transmitted signals behave statistically as a Gaussian process and therefore overestimates the amount of NLI noise generated when compared to the transmission of modulated signal using square QAM constellations. However, the increase observed in the NLI noise from the experimental data follows the same logarithmic relationship with the signal bandwidth. The most significant increase in the NLI noise power occurs as the bandwidth is increased from a single channel of 40 GHz to 280 GHz, contributing to approximately 50% of the total NLI noise generated in the transmission of 7.3 THz. This is because as the signal bandwidth is increased, the outer channels with the largest frequency separation with respect to the evaluated channel, contribute less to the total NLI noise power due dispersion induced walk-off effects. Additionally, due to the use of SS-ASE to load the bandwidth beyond the 7 modulated channels, the accuracy of the model is improved in relationship to the experimental data as the larger fraction of the transmitted bandwidth corresponds to SS-ASE.

C. The Effect of NLI on the Communication System

After analysing the impact NLI will have on the SNR after transmission through optical fibre, the next step was to investigate the effect NLI has on the optical communication system performance. The goal of a communication system is to transmit information reliably between two or more parties. The mutual information between the received and transmitted symbols quantifies the maximum rate at which a system can reliably transmit information for a given modulation format, and it is becoming the performance metric of choice to design and characterize optical systems [26], [27].

From Fig. 4 can be seen that NLI noise decreases the received SNR as the total transmitted bandwidth increases, leading to a reduction of the maximum achievable rates of the system. Using (4) and (1) it is possible to relate the growth of the NLI noise to the decrease of the achievable rate. Fig. 6 shows the MI of the received channel plotted against the total transmitted bandwidth for a transmission distance of 1010 km. It can be seen that when a single 64-QAM channel is transmitted, information rate of 9.4 bits/symbol can be achieved. Increasing the number of transmitted channels from 1 to 7 reduces the MI of the central channel to 9 bits/symbol due to the additional NLI noise generated during transmission. Finally, when the total transmitted bandwidth is increased up to 7.3 THz the MI is further decreased to 8.1 bits/symbol. This corresponds to a reduction in the information rate of approximately 15% for the modulation format and distance used.

The achievable rates in a communication system depend on the total transmission distance due to the accumulation of noise. To study the impact of NLI noise as a function of distance, MI of a single 40 GBd channel, centred at 1550 nm within a 7.3 THz

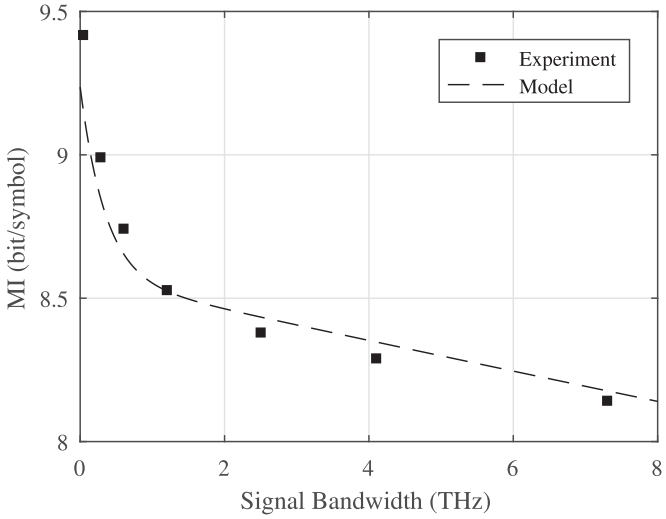

Fig. 6. Impact of the NLI on the achievable rates at a transmission distance of 1010 km. Markers represent experimental data and solid line represents model predictions.

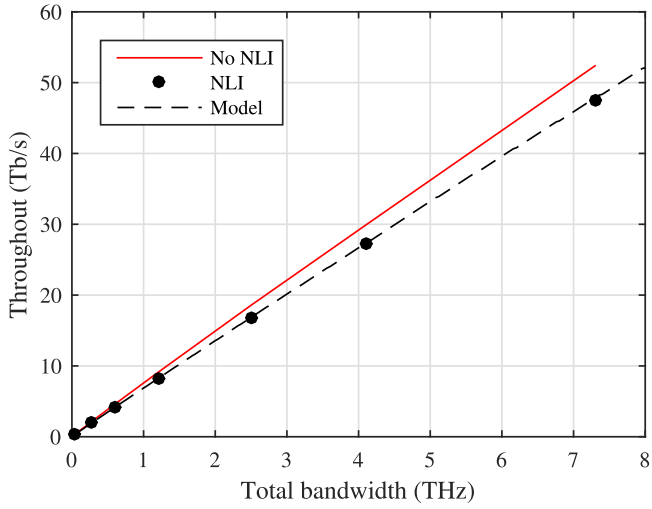

Fig. 8. Total system throughput as a function of the transmitted bandwidth. Red line represents a system not impaired by NLI noise, obtained from the reiceved OSNR, and black line corresponds to the transmission system. Markers represent experimental data.

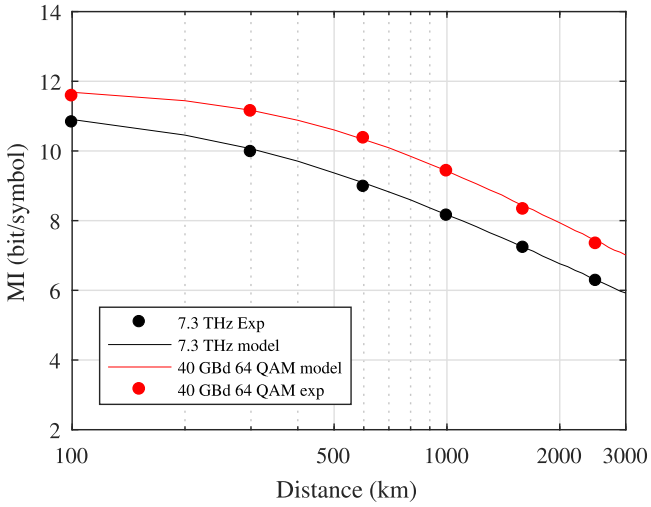

Fig. 7. Achievable information rates as a function of transmitted distance for transmission of a single channel (red) and 7.3 THz total bandwidth (black). Markers correspond to experimental data and lines to the model predictions.

total bandwidth, was measured for different transmission distances, with the results shown in Fig. 7. At short transmitted distances, below 300 km, there is only a small difference between the performance for both bandwidths (0.75 bit/symbol), since the system is largely dominated by the transceiver limited SNR. It can be seen that achievable rates converge to the back-to-back performance for short distances. At longer transmission distances, the central channel MI is reduced for wide bandwidth transmission due to the increased NLI noise and there is a difference of 1.1 bit/symbol after 2500 km transmission, corresponding also to a 15 % decrease in the achievable information rate. It is expected that this difference will be maintained for longer transmission distances. Due to the relationship between SNR and MI, we find the accuracy of the model improved when used to predict the achievable rates of the system, as can be seen from Fig. 7, with the largest observed difference between the model and the experiment of 0.2 bit/symbol for the transmission of a single channel. Therefore, as achievable throughput is ultimately the quantity of interest, it can be concluded that the GN model is particularly accurate at estimating central channel performance at optimum launch power, even in C+L-band transmission systems.

Finally, the trade-off between the use of large optical bandwidth and the accumulation of NLI noise was analysed using the estimated achievable rates[1]. It is well known that the capacity of an AWGN channel is given by $C = 2 \times B \times log_2(1 + \text{SNR})$ [28], where B corresponds to the signal bandwidth. Ideally, in the absence of fibre nonlinearities, increasing the transmission bandwidth would allow a linear growth in the system throughput. However, due to the accumulation of NLI noise as the bandwidth is extended, the MI of the transmitted channels is reduced resulting in a sublinear scaling of the system throughput. In order to address this nonlinear penalty on system throughput, Fig. 8 shows the system throughput as a function of the transmitted signal bandwidth after 1010 km. The red line illustrates the throughput obtained from the measured received OSNR for each value of the transmitted bandwidth at optimum signal launch power; this represents a system not affected by nonlinear impairments. To calculate this, the received SNR was estimated from the OSNR using the back-to-back characterization from Fig. 3, and subsequently, the MI was calculated from the estimated SNR. The degradation of the system throughput due to NLI noise was studied from the experimental data after transmission, with the black line showing the total throughput

[1]This analysis was carried out assuming that all the transmitted WDM channels are equally affected by NLI noise and ASE noise. This assumption is not true in a real transmission system where the noise figure of the optical amplifiers can vary as a function of wavelength and the outer channels experience less NLI noise, however it provides sufficiently useful insight to study how the system throughput behaves in a transmission system impaired by NLI.

as a function of bandwidth. For the transmission of a single channel the throughput is reduced by 6% from 317 to 298 Gb/s. Due to the increase of NLI noise this is further increase for the transmission of larger bandwidths. For a transmitted bandwidth of 7.3 THz the data throughput is decreased from 52 to 47.5 Tb/s due to nonlinear effects, corresponding to a reduction of approximately 10%. A number of digital and optical techniques have been explored to mitigate the impairments introduced by NLI noise, which would enable an increase in the received SNR. However, due to the logarithmic relationship between the system capacity and the SNR, the benefits of these techniques are limited. Increasing the transmission bandwidth, on the other hand, despite the sublinear scaling introduced by the accumulation of NLI noise, offers an attractive solution to increase the throughput in optical communication systems.

D. On the Stimulated Raman Scattering Effect

Although an increase in the transmission bandwidths appears to be a promising solution to increase the throughput of optical communication systems, it is important to be aware that additional nonlinear effects are likely to have a significant impact as the optical bandwidths are further increased. One major issue is stimulated Raman scattering (SRS) between the transmitted signals. SRS is a nonlinear process where power from one optical field is transferred to another, whose frequency is downshifted by an amount determined by the vibrational modes of the medium [29]. In silica fibres the Raman gain spectrum has a maximum at a frequency shift of approximately at 13 THz. The power difference experienced by different wavelengths due to the SRS effect was measured for the system under study after the first fibre span for the transmission of 7.3 THz of bandwidth. The analysed wavelengths were 1528, 1550 and 1591 nm, corresponding to the two most outer channels of the transmitted spectrum (1528 & 1591 nm) and the channel under evaluation centred at 1550 nm. The obtained results are shown in Fig. 9 as a function of signal input power into the fibre. It can be seen that the power difference, either gain or loss, experienced by the channels due to the SRS effect is increased as the signal power becomes higher. For the channel centred at 1550 nm only a small fraction of the power is lost due to Raman scattering to higher wavelengths. At optimum power, 2 dBm/channel, the signal power at 1550 is decreased by 0.35 dB. This implies that the performance of this channel will not be strongly affected by the SRS effect. However, the power difference between the outer channels becomes significant as the input power is increased. It can be seen that at 1528 nm the optical power is decreased, while at 1591 nm the power experiences gain from the scattered light from shorter wavelengths. Overall a tilt in the optical spectrum of approximately 2 dB is present at optimum signal power. This suggests that the effect of noise and power transfer due to SRS on the channels located at the edges of the transmitted spectrum, specially as the transmitted bandwidths grow larger, will have a significant impact on the total system throughput introducing further limitations beyond the NLI noise induced impairments, leading to larger variations on received SNR for different channels. However, experimental demonstrations and theoretical results for high capacity transmission have proposed and implemented the use of coded modulation with variable spectral efficiencies across the channels in order to maximise the transmission capacity [30], [31] to overcome this impairments.

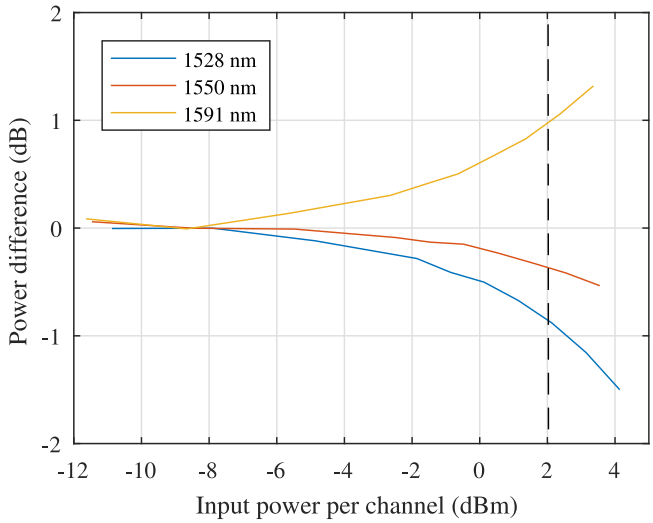

Fig. 9. Power difference due to SRS effect experienced by different wavelengths as a function of signal launch power. Blue, orange and yellow lines represent the power variations for 1528, 1550 and 1591 nm. Dashed vertical line corresponds to the optimum signal power of the system.

IV. Conclusion

The accumulation of nonlinear impairments was experimentally and theoretically studied for long haul transmission systems with signal bandwidths up 7.3 THz. It was observed that SNR monotonically decreased with signal bandwidth at optimum launch power, in line with predictions from the GN model. The NLI noise was experimentally confirmed to grow following a logarithmic law for all the studied bandwidths. The potential throughput of the transmission system under test was reduced from 52 to 47.5 Tb/s due to the effect of nonlinear distortions, which corresponds to a reduction of the achievable rates of approximately 10%. Even though the theoretical models are able to predict this behaviour, this is the first comprehensive experimental study analysing this effect. Using this metric we conclude that even with the monotonic increase of NLI with signal bandwidth, increasing the signal bandwidth still appears among the most promising solutions to continue the development of high capacity systems. Finally, to continue the progress of high capacity systems using large transmission bandwidths special attention will be needed towards the SRS effect in order to design system beyond the current used transmission bandwidths.

Acknowledgment

The authors would like to thank Dr. S. Makovejs and Corning Inc., for the loan of the Corning Vascade EX2000 fibre.

REFERENCES

[1] M. Yamada, H. Ono, T. Kanamori, S. Sudo, and Y. Ohishi, "Broadband and gain-flattened amplifier composed of a 1.55 um-band and a 1.58 um-band er3+-doped fibre amplifier in a parallel configuration," *Electron. Lett.*, vol. 33, no. 8, pp. 710–711, Apr. 1997.

[2] H. Kidorf, K. Rottwitt, M. Nissov, M. Ma, and E. Rabarijaona, "Pump interactions in a 100-nm bandwidth raman amplifier," *IEEE Photon. Technol. Lett.*, vol. 11, no. 5, pp. 530–532, May 1999.

[3] S. V. Firstov *et al.*, "Bismuth-doped optical fiber amplifier and watt-level CW laser for the spectral region 1600–1800 nm," in *Proc. Opt. Fiber Commun. Conf. Exhib.*, Mar. 2016, Paper no. M3D.6.

[4] Y. Jung *et al.*, "Silica-based thulium doped fiber amplifiers for wavelengths beyond the l-band," in *Proc. Opt. Fiber Commun. Conf. Exhib.*, Mar. 2016, Paper no. M3D.5.

[5] J. X. Cai *et al.*, "70.4 tb/s capacity over 7,600 km in c+l band using coded modulation with hybrid constellation shaping and nonlinearity compensation," in *Proc. Opt. Fiber Commun. Conf. Exhib.*, Mar. 2017, Paper no. Th5B.2.

[6] L. E. Nelson, X. Zhou, B. Zhu, M. F. Yan, P. W. Wisk, and P. D. Magill, "All-raman-amplified, 73 nm seamless band transmission of 9 tb/s over 6000 km of fiber," *IEEE Photon. Technol. Lett.*, vol. 26, no. 3, pp. 242–245, Feb. 2014.

[7] P. Poggiolini, "The GN model of non-linear propagation in uncompensated coherent optical systems," *J. Lightw. Technol.*, vol. 30, no. 24, pp. 3857–3879, Dec. 2012.

[8] R. Dar, M. Feder, A. Mecozzi, and M. Shtaif, "Properties of nonlinear noise in long, dispersion-uncompensated fiber links," *Opt. Express*, vol. 21, no. 22, pp. 25 685–25 699, Nov. 2013.

[9] P. Poggiolini, G. Bosco, A. Carena, V. Curri, Y. Jiang, and F. Forghieri, "The GN-model of fiber non-linear propagation and its applications," *J. Lightw. Technol.*, vol. 32, no. 4, pp. 694–721, Feb. 2014.

[10] A. Nespola *et al.* "GN-model validation over seven fiber types in uncompensated PM-16QAM nyquist-WDM links," *IEEE Photon. Technol. Lett.*, vol. 26, no. 2, pp. 206–209, Jan. 2014.

[11] L. Galdino *et al.*, "Experimental demonstration of modulation-dependent nonlinear interference in optical fibre communication," in *Proc. 42nd Eur. Conf. Opt. Commun.*, Sep. 2016, Paper no. Th.1.A.2.

[12] R. Pastorelli *et al.*, "Investigation of the dependence of non-linear interference on the number of WDM channels in coherent optical networks," in *Proc. 38th Eur. Conf. Exhib. Opt. Commun.*, Sep. 2012, Paper no. We.2.C.2.

[13] J. X. Cai *et al.*, "Transmission performance of coded modulation formats in a wide range of spectral efficiencies," in *Proc. Opt. Fiber Commun.*, Mar. 2014, Paper no. M2C.3.

[14] G. Saavedra *et al.*, "Experimental investigation of nonlinear signal distortions in ultra-wideband transmission systems," in *Proc. Opt. Fiber Commun. Conf. Exhib.*, Mar. 2017, Paper no. W1G.1.

[15] D. J. Elson, L. Galdino, R. Maher, R. I. Killey, B. C. Thomsen, and P. Bayvel, "High spectral density transmission emulation using amplified spontaneous emission noise," *Opt. Lett.*, vol. 41, no. 1, pp. 68–71, Jan. 2016.

[16] D. J. Elson *et al.*, "Investigation of bandwidth loading in optical fibre transmission using amplified spontaneous emission noise," *Opt. Express*, vol. 25, no. 16, pp. 19 529–19 537, Aug 2017. [Online]. Available: http://www.opticsexpress.org/abstract.cfm?URI=oe-25-16-19529

[17] J. Cho *et al.*, "Trans-atlantic field trial using probabilistically shaped 64-QAM at high spectral efficiencies and single-carrier real-time 250-gb/s 16-QAM," in *Proc. Opt. Fiber Commun. Conf. Exhib.*, Mar. 2017, Paper no. Th5B.3.

[18] M. J. Ready and R. P. Gooch, "Blind equalization based on radius directed adaptation," in *Proc. Int. Conf. Acoust., Speech, Signal Process.*, Apr. 1990, vol. 3, pp. 1699–1702.

[19] D. Godard, "Self-recovering equalization and carrier tracking in two-dimensional data communication systems," *IEEE Trans. Commun.*, vol. 28, no. 11, pp. 1867–1875, Nov. 1980.

[20] T. Pfau, S. Hoffmann, and R. Noé, "Hardware-efficient coherent digital receiver concept with feedforward carrier recovery for M-QAM constellations," *J. Lightw. Technol.*, vol. 27, no. 8, pp. 989–999, Apr. 2009.

[21] I. Fatadin, S. J. Savory, and D. Ives, "Compensation of quadrature imbalance in an optical QPSK coherent receiver," *IEEE Photon. Technol. Lett.*, vol. 20, no. 20, pp. 1733–1735, Oct. 2008.

[22] G. Liga, A. Alvarado, E. Agrell, and P. Bayvel, "Information rates of next-generation long-haul optical fiber systems using coded modulation," *J. Lightw. Technol.*, vol. 35, no. 1, pp. 113–123, Jan. 2017.

[23] L. Galdino *et al.* "On the limits of digital back-propagation in the presence of transceiver noise," *Opt. Express*, vol. 25, no. 4, pp. 4564–4578, Feb. 2017.

[24] A. Carena, G. Bosco, V. Curri, Y. Jiang, P. Poggiolini, and F. Forghieri, "EGN model of non-linear fiber propagation," *Opt. Express*, vol. 22, no. 13, pp. 16 335–16 362, Jun. 2014.

[25] R. Dar, M. Feder, A. Mecozzi, and M. Shtaif, "Accumulation of nonlinear interference noise in fiber-optic systems," *Opt. Express*, vol. 22, no. 12, pp. 14 199–14 211, Jun. 2014.

[26] R. Maher, A. Alvarado, D. Lavery, and P. Bayvel, "Increasing the information rates of optical communications via coded modulation: a study of transceiver performance," *Sci. Rep.*, vol. 6, no. 1, 2016, Art. no. 21278.

[27] R. J. Essiambre, G. Kramer, P. J. Winzer, G. J. Foschini, and B. Goebel, "Capacity limits of optical fiber networks," *J. Lightw. Technol.*, vol. 28, no. 4, pp. 662–701, Feb. 2010.

[28] C. E. Shannon, "A mathematical theory of communication," *Bell Syst. Tech. J.*, vol. 27, no. 4, pp. 623–656, Oct. 1948.

[29] G. P. Agrawal, *Nonlinear Fiber Optics*. New York, NY, USA: Academic, 2007.

[30] J. X. Cai *et al.* "49.3 tb/s transmission over 9100 km using c+l EDFA and 54 tb/s transmission over 9150 km using hybrid-raman EDFA," *J. Lightw. Technol.*, vol. 33, no. 13, pp. 2724–2734, Jul. 2015.

[31] D. Semrau, R. Killey, and P. Bayvel, "Achievable rate degradation of ultra-wideband coherent fiber communication systems due to stimulated raman scattering," *Opt. Express*, vol. 25, no. 12, pp. 13 024–13 034, Jun. 2017.

Authors' biographies not available at the time of publication.